



HAL
open science

Simulation of Orowan's mechanism using dislocation dynamics based on the non-singular elastic theory

M. Shukeir, L. Dupuy, B. Devincre

► **To cite this version:**

M. Shukeir, L. Dupuy, B. Devincre. Simulation of Orowan's mechanism using dislocation dynamics based on the non-singular elastic theory. 2020. cea-02339875

HAL Id: cea-02339875

<https://cea.hal.science/cea-02339875>

Preprint submitted on 18 Mar 2020

HAL is a multi-disciplinary open access archive for the deposit and dissemination of scientific research documents, whether they are published or not. The documents may come from teaching and research institutions in France or abroad, or from public or private research centers.

L'archive ouverte pluridisciplinaire **HAL**, est destinée au dépôt et à la diffusion de documents scientifiques de niveau recherche, publiés ou non, émanant des établissements d'enseignement et de recherche français ou étrangers, des laboratoires publics ou privés.

Simulation of Orowan's mechanism using dislocation dynamics based on the non-singular elastic theory

Malik Shukeir^a, Laurent M Dupuy^{a,*}, Benoit Devincere^b

^a*Den-Service de Recherches Métallurgiques Appliquées (SRMA), CEA, Université Paris-Saclay, F-91191, Gif-sur-Yvette, France*

^b*Lab. d'Étude des Microstructures, CNRS, ONERA, 29, avenue de la division Leclerc, BP 72, 92322, Châtillon, France*

Abstract

The motion of dislocations, as computed by dislocation dynamics simulations, depends on the underlying energetic model casted within a continuum approach. This model is nevertheless still debated due to the difficulty in capturing the behavior of the atoms in the core of dislocations. Here, we investigate the influence of the corresponding material core parameters on the outcome of dislocation dynamics simulations of the Orowan bypassing mechanism. A parametric study first reveals a large dispersion of the critical Orowan stress. Within a semi empirical approach, a new predictive equation is then motivated to encompass the core parameters, and extend the original formula proposed by Bacon, Kocks and Scattergood. Emphasizing the need to carefully selecting these parameters, we finally advocate the use of the Orowan mechanism to calibrate dislocation dynamics simulations.

Keywords: Dislocation dynamics simulation, Orowan mechanism, Non-singular elastic theory

1. Introduction

Dislocation Dynamics (DD) simulations rely inherently on a continuum description of dislocations based on the linear elasticity (e.g. [1]), whose accuracy in capturing the strain and stress fields around dislocations has been proven experimentally over the years (e.g. [2]). As such, this simulation method nevertheless fails at describing the discrete atomic positions in the immediate vicinity of a dislocation, and consequently its energy. As pointed out by Bulatov and Cai [3], this remark holds even for *non-singular* elasticity models [4, 5, 6] where the stress field remains finite in the core of the dislocation. Most DD simulations therefore partition the total energy of a dislocation into an elastic and a core-energy contribution [7], the latter being added to account for whatever is left by the former in the dislocation core. Despite noticeable efforts in feeding atomistic information to these models [8, 9, 10], limited efforts have been made so far to identify the relevant parameters on atomistic data, nor to assess their influence on classical dislocation mechanisms such as the Orowan process. The objective of this study is therefore to address this issue and provide guidelines to choose the corresponding parameters.

*Corresponding author. Tel.: +33-169085345

Email address: laurent.dupuy@cea.fr (Laurent M Dupuy)

Among the various approaches used in current DD codes ([7, 11, 12, 13, 14, 15]) to account for dislocations total strain energy, the choice was made here to use the isotropic non-singular elastic model of Cai *et al.* [6] in combination with a basic core energy model. In the absence of a comprehensive atomistic data base, the latter is simply based on the orientation dependent line tension approach [16]. The former offers many mathematical and computational advantages, and is currently widely used. As we will discuss it latter, these choices restraint the relevant energy parameters to two values. We therefore believe that this study should be of use and applicable to almost all the DD codes.

The Orowan mechanism [17] was selected in this study as our reference case. This mechanism, which is the bypassing of strong precipitates made by a dislocation line moving in a given glide plane, was preferred to other elementary phenomena for the following reasons. First, it has an important impact on plastic strain hardening [18, 19] and has been widely studied in the literature at the mesoscopic scale using dislocation dynamics [20, 21, 22, 23, 24]. Secondly, it does not rely on unphysical arbitrarily pinned dislocation ends by contrast with the Frank-Read source [25] and can therefore be simultaneously investigated using molecular dynamics (MD) [19, 26, 27]. Finally, the Orowan mechanism questions simultaneously the underlying dislocation strain energy through its *effective line tension* and the stress required to bow out the side arms of the dislocation, as well as its *stress field* and the corresponding elastic interaction between the arms as the dislocation bypasses the precipitates [20]. Previous studies investigated the effect of precipitate size and distribution on the mechanical properties, but to our knowledge no study investigated in a systematic manner the influence of the dislocation strain energy parameters used in DD simulations.

This paper is organized as follows. In the next section we present a brief overview of dislocation elastic theory and parameters appearing in the dislocation strain energy definition used in most DD simulations, as well as the standard model used to predict Orowan stress in the case of impenetrable obstacles. In section (3), we describe the details of the parametric study performed in this article. The corresponding results are presented in section (4). The last section is dedicated to a discussion and concluding remarks.

2. Theoretical background

In linear theory of elasticity, it is convenient to split the total energy of a dislocation into two separate terms, one for the long range elastic field and the other for the core energy [2].

$$E_{total} = E_{elastic} + E_{core} \quad (1)$$

Most of the total energy of a dislocation comes from the elastic strain energy contribution, while the core energy is reported to constitute a few percent of the total elastic strain energy [28, 1]. Assuming isotropic elasticity, the self-energy per unit length of a dislocation stored in a cylindrical ring of inner radius r_0 (core radius) and outer radius R_0 in the case of infinite straight dislocations is

$$E_{elastic}^{inf} = \frac{\mu b^2}{4\pi(1-\nu)} (1 - \nu \cos^2 \theta) \ln\left(\frac{R_0}{r_0}\right) \quad (2)$$

where μ is the isotropic shear modulus, b is the Burgers vector and ν is the Poisson's ratio. The dislocation character term θ is the angle between the Burgers vector and the tangent vector along the dislocation line. From Equation (2), we simply see that the elastic energy of a dislocation

depends on i) the dislocation core definition via r_0 , ii) the initial and boundary condition via the definition of R_0 and iii) the dislocation character (edge or screw) via the pre-logarithmic energy constant [2, 1].

Because of the inability of the elastic theory to represent the core energy of a dislocation, and in the absence of comprehensive atomistic information, the choice was made here to define the core energy as being directly proportional to the elastic energy per unit length of an infinite straight dislocation through a single parameter, α_{core} , such as:

$$E_{core} = \alpha_{core} E_{elastic}^{inf} \quad (3)$$

This approach is consistent with several available atomistic studies (e.g. [29, 1]) in which the core energy amounted to a few percent of the elastic energy. For convenience, we introduce at this point a term called the core energy parameter ζ_{core} . The latter constant quantity take the form:

$$\zeta_{core} = \alpha_{core} \ln\left(\frac{R_0}{r_0}\right) \quad (4)$$

The core energy can therefore be written as:

$$E_{core} = \zeta_{core} \frac{\mu b^2}{4\pi(1-\nu)} (1 - \nu \cos^2 \theta) \quad (5)$$

The driving force controlling dislocation dynamics is mainly a function of the loading stress, and internal stresses generated by each dislocation line. The calculation of the internal stress field associated with an ensemble of curved dislocations needs integrating equation [2, 30, 6]:

$$\begin{aligned} \sigma_{\alpha\beta} = & \frac{\mu}{8\pi} \oint \partial_i \partial_p \partial_p R [b_m \varepsilon_{im\alpha} dx'_\beta + b_m \varepsilon_{im\beta} dx'_\alpha] \\ & + \frac{\mu}{4\pi(1-\nu)} \oint b_m \varepsilon_{imk} (\partial_i \partial_\alpha \partial_\beta R - \delta_{\alpha\beta} \partial_i \partial_p \partial_p R) dx'_k \quad (6) \end{aligned}$$

where R is the distance between points α and β on the dislocation line and ε_{ijk} is Levi-Civita notation.

A major difficulty in calculating the stress field of dislocations is related to the fact that Equation (6) is divergent when R approaches zero. Different solutions have been proposed to eliminate such singularity as in [5, 6, 31]. Among those solutions, the one proposed by Cai *et al.* [6] features some specifications which makes it convenient for DD simulations. In brief, it modifies the singular stress field solution through a mathematical transformation where R in Equation (6) is replaced by $R_a = \sqrt{R^2 + a_0^2}$. This transformation implies the definition of a new regularization parameter a_0 coined as the dislocation core width parameter.

Hence, the dislocation strain energy definition used in this study reduces to two major parameters: the dislocation core width parameter a_0 and the core energy parameter ζ_{core} . In order to assess the impact of these parameters, we perform DD simulations on the Orowan mechanism.

In a seminal work, Bacon *et al.* [20] investigated the bypass of a periodic row of impenetrable spherical obstacles by an infinite dislocation with the Orowan's mechanism [17]. From an

analysis of the influence of the obstacle size (D) and the inter-obstacle distance (L) on the flow stress, they defined the following equation (hereinafter referred to the BKS model):

$$\tau = A \frac{\mu b}{L} [\ln \bar{D} + B] \quad (7)$$

In Equation (7), A is a pre-logarithmic factor that depends on the character of the dislocation. $A = 1$ and $A = 1/(1 - \nu)$ for edge and screw dislocations, respectively. B is a fitting parameter evaluated to 0.7 in the BKS paper. This model equation is widely used in the literature as a reference for Orowan-like interactions [23, 24].

3. Simulation technique

Simulations were carried out using NUMODIS [15, 32], a 3D nodal dislocation dynamics (DD) code based on the isotropic elastic theory of dislocations. Dislocation lines are represented by a set of nodes, interconnected by straight segments nodes, whose properties are their Burgers vector and their glide plane.

This study is performed on a single crystal of BCC Iron at 300K. At this temperature, the lattice parameter equals 0.2855 nm , b the Burgers vector of slip systems $^{1/2}\langle 111 \rangle(11\bar{0})$ equal 0.2475 nm and the shear modulus μ equal 63 GPa. The x , y and z axes of the simulated volume are oriented in the $[111]$, $[\bar{1}\bar{1}2]$ and $[11\bar{0}]$ crystallographic directions, respectively. Periodic boundary conditions are applied in the $[111]$ and $[\bar{1}\bar{1}2]$ directions, while no particular conditions are applied to the boundary surfaces in the $[11\bar{0}]$ direction since they are normal to the dislocation glide direction.

Following a robust methodology previously used to simulate the Orowan process [24, 23, 33], one $^{1/2}\langle 111 \rangle(11\bar{0})$ edge or screw dislocation is introduced in the periodic volume in front of an impenetrable spherical obstacle with diameter D and cut by the dislocation glide plane at its center (Figure 1). This obstacle is considered as an incoherent inclusion, whose elastic properties are equal to the surrounding crystal. No specific stress field is therefore associated with the obstacle. The spacing L between periodic images of the obstacle is varied by changing the size of the simulation box along the direction parallel to the dislocation line. The dimension of the simulated volume in the glide direction is systematically adjusted to allow for Orowan loop formation before the dislocation line reach the boundary of the periodic volume. The z -axis is systematically adjusted to be three times the obstacle diameter.

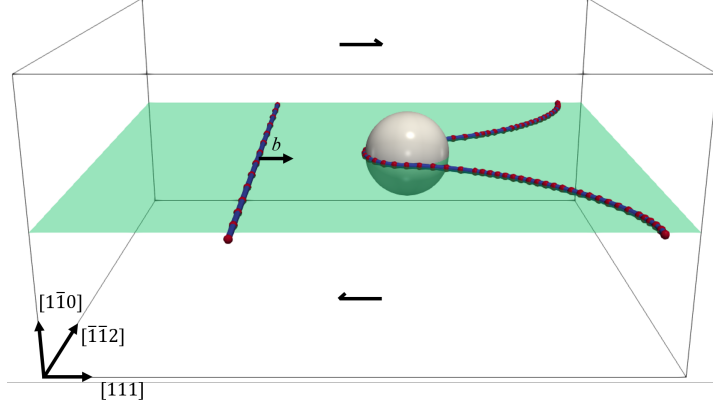


Figure 1: Illustration of the DD Simulation volume. The green surface represents the glide plane of the mobile dislocation, while arrows at the top and bottom surfaces indicate the direction of the applied shear stress. The straight dislocation represents the initial dislocation configuration while the curved one is the critical configuration observed before the formation of the Orowan loop.

Pure shear stress is applied in the b direction to impose a constant strain rate which corresponds to a constant dislocation velocity in the glide plane close to $3m/s$. For reasons of simplicity and to allow for comparison with previous computations made in FCC materials, we consider in the simulations a simple linear over-damped mobility law similar to [34], in the form:

$$v_s = \frac{\tau b}{B} \quad (8)$$

where τ is the effective resolved shear stress and B is a viscosity coefficient set to $8 * 10^{-5}$ Pa.s. The latter quantity accounts for dissipating processes like dislocation-phonon interactions. All simulations are done in a *quasi-static* condition and tests have been made to verify that the viscosity coefficient value has no influence on the computed critical stress. Here, it must be noted that although thermally activated bypassing mechanisms are reported in the literature in case of small obstacles, for reasons of simplicity no thermally activated dislocation property like, dislocation cross-slip or climb, are considered in the present simulations. All the material parameters used in the DD simulations are consistent with prior molecular dynamics simulations found in [35, 36, 37].

In order to investigate the influence of the two core parameters, a parametric study of the Orowan mechanism was conducted. The range of the many combinations we tested are summarized in Table (1).

4. Simulation results

The results of all the calculations of the Orowan critical stress we conducted are plotted in Figure (2). For comparison with the BKS model, the Orowan stress is plotted as a function of the harmonic mean of the inter-obstacle spacing and obstacle diameter, $(L^{-1} + D^{-1})^{-1}$. A large dispersion of the values is found when changing the parameters controlling the dislocation elastic energy. In the edge dislocation case, and for different values of the harmonic mean, an increase of 100% in the critical stress is observed. Such dispersion is found to be even more important

Table 1: Energy and geometrical simulation parameters we explored to calculate the Orowan stress.

Parameter	Symbol	Range	Unit
Regularization parameter	a_0	1.5, 2.5, 4.0, 5.0	Å
Core energy parameter	ζ_{core}	0.09, 0.43, 0.86, 1.28	-
Poisson ratio	ν	0.0, 0.2, 0.33, 0.435, 0.495	-
Inter-obstacle distance	L	100.0, 316.2, 1000.0	b
Obstacle size	D	10.0, 31.62, 100, 316.2	b

in the case of screw dislocations, where the critical stress increases of approximately 280% for different sets of parameters.

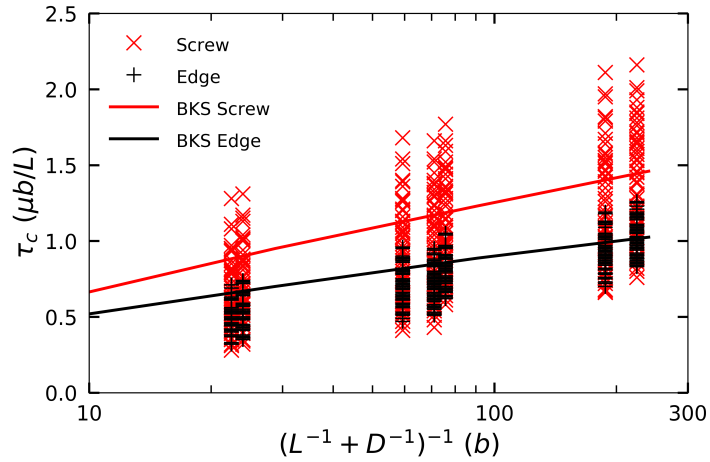


Figure 2: Result of the Orowan stress calculation with screw and edge dislocations in reduced units. Each mark is a unique combination of the parameters reported in Table (1). Continuous lines are the prediction of the BKS model (Equation 7).

To understand the effect of each parameter, our simulation results are now plotted separately by fixing all but one of the energy parameters. In Figure (3), we show the effect of changing the Poisson ratio while the other simulation parameters are $L = 1000b$ (247 nm), $D = 100b$ (24.7 nm), $a_0 = 0.4$ nm and $\zeta_{core} = 0.86$.

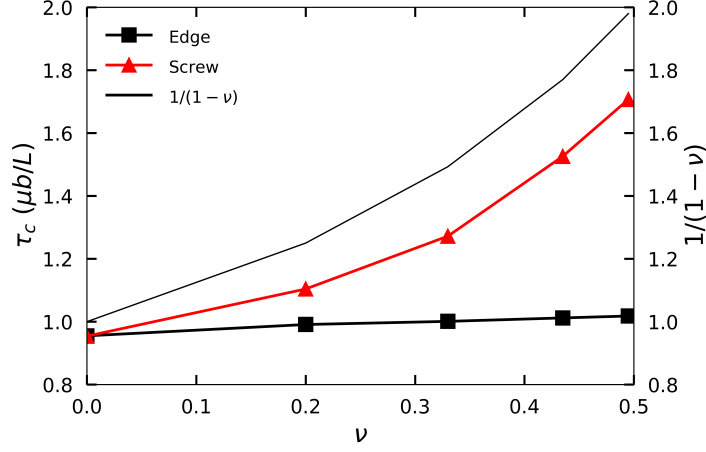


Figure 3: Variation of the Orowan stress as function of the Poisson ratio for screw and edge dislocations. Other simulation parameters are $L = 1000b$ (247 nm), $D = 100b$ (24.7 nm), $a_0 = 0.4$ nm and $\zeta_{core} = 0.86$.

The critical stress of an edge dislocation is observed to be quasi-independent of the Poisson ratio ν , while a non-linear dependence of the form $1/(1-\nu)$ is observed in the case of a screw dislocation. This observation is in agreement with the line tension model proposed by De Wit [16] that accounts for the effect of the dislocation character and the simulation results first reported in [20]. Figure (3) as well shows that when ν equals zero, the Orowan stress is independent of the dislocation character and the Orowan stress is independent of the dislocation line character as expected.

The second analyzed simulation parameter is the core energy parameter ζ_{core} . As shown in Equation (3), α_{core} has a linear influence on the total strain energy of the dislocation and therefore on dislocation line tension. Hence, if the ratio $\ln(R_0/r_0)$ is constant, a linear dependence is observed on the Orowan stress as function of ζ_{core} . The same tendency is observed on screw and edge dislocations (see Figure 4). More precisely, increasing ζ_{core} by a factor of 10 increases the critical stress by about 33%. This reveals a fairly high dependence of DD simulations on the definition of the dislocation core energy. This point has been probably overlooked in several existing studies.

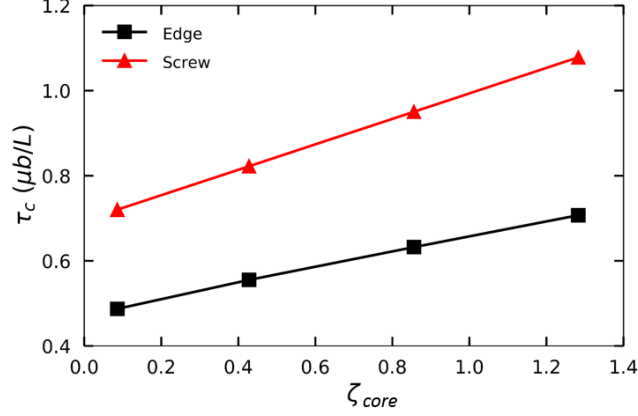


Figure 4: Variation of the Orowan stress as function of the core energy parameter ζ_{core} . Other simulation parameters are set to $L = 100b$ (24.7 nm), $D = 10b$ (2.47 nm), $a_0 = 0.15$ nm and $\nu = 0.435$.

With regard to the effect of a_0 , the regularization parameter, we see that the Orowan stress has an inverse logarithmic dependence on this parameter. Such behavior is shown in Figure (5), where other simulation parameters are $L = 1000b$ (2470 Å), $D = 100b$ (247 Å), $\zeta_{core} = 0.86$ and $\nu = 0.435$.

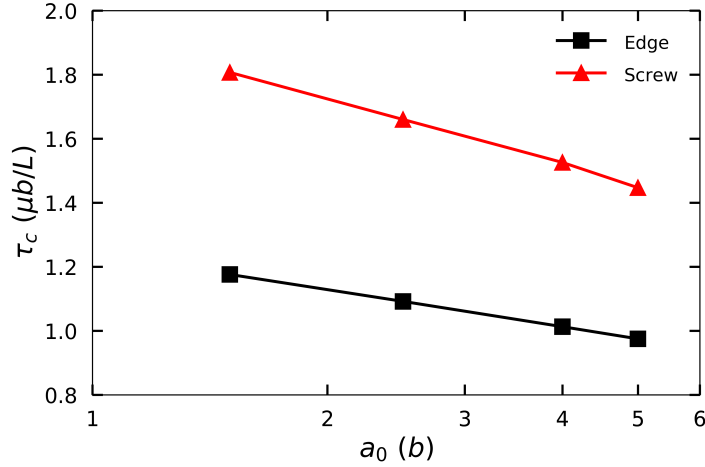


Figure 5: Variation of the normalized Orowan stress as function of core width parameter a_0 . Other simulation parameters are set to $L = 1000b$ (2470 Å), $D = 100b$ (247 Å), $\zeta_{core} = 0.86$ and $\nu = 0.435$.

The inversely logarithmic dependence observed in Figure (5) can be motivated by the dislocation energy expression computed by Cai *et al.* [6] in the context of the non-singular theory. Indeed, the core width parameter a_0 appears in the denominator of the logarithmic term, as if r_0 was replaced by a_0 in equation (2). Consequently, the simulated Orowan stress is decreased by approximately 18% and 16%, for screw and edge dislocations respectively, when increasing the

regularization parameter a_0 by a factor of 3. This result raises doubts about the relevance of DD simulations, which use regulation parameters 10 to 100 times larger than the core radius of the dislocations defined by atomic simulations for computational reasons.

Lastly, we show that in agreement with the BKS model for a given set of simulation parameters, the Orowan stress is logarithmically dependent on the harmonic mean of inter-obstacle distance and obstacle size. Such result is presented in Figure (6) with a set of simulation parameters ($a_0 = 4.5$ nm, $\zeta_{core} = 0.86$ and $\nu = 0.33$) and is in good agreement with the solution found in previous simulations. As discussed in [20], the evolution of the Orowan stress is here well described with the help of a harmonic mean between the inter-obstacle distance L and the obstacle diameter D . When L is much larger than D the average tends to L and the required stress to overcome the precipitate decreases, since the line tension of a dislocation is inversely proportional to its length, and vice versa.

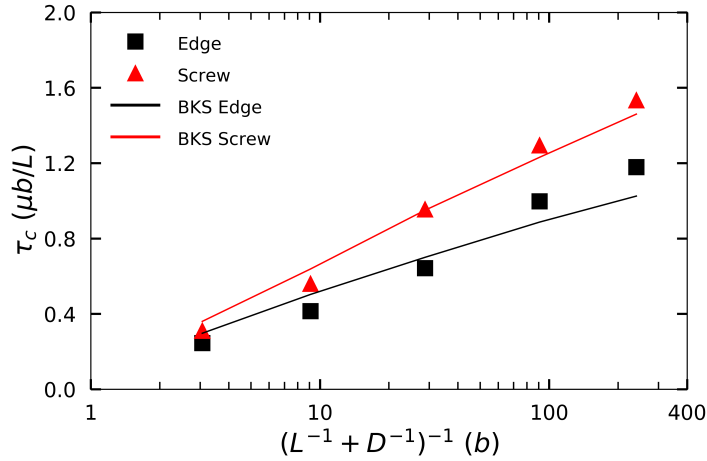


Figure 6: Normalized Orowan stress vs the harmonic mean of inter-obstacle length and obstacle diameter. The simulation parameters controlling the elastic energy are set to $a_0 = 4.5$ nm, $\zeta_{core} = 0.86$ and $\nu = 0.33$. The continuous lines are the BKS model prediction with the fit parameter calculated in [20].

5. Discussion and concluding remarks

In this work, we studied in α -iron the interaction of infinite $1/2\langle 111 \rangle(11\bar{0})$ screw and edge dislocations with a periodic array of impenetrable obstacles of different size and spacing. These configurations are standard simulation problems previously used to study the Orowan mechanism with MD and DD simulations. The reported results are in good agreement with previous studies, but reveal a large dispersion of results when changing the simulation parameters used to define the dislocation strain energy. More specifically, for the different solutions of simulation parameters, the calculated Orowan stress can vary by 100% and 280% for edge and screw dislocations, respectively.

In order to reveal the collective effect of the studied parameters to the Orowan stress, we propose to combine them in a new equation. This equation represents the sum of two contributions. It reflects the strain energy decomposition into elastic and core energy contributions (see

Equation 1). The first contribution is similar to the one defined in the BKS model, but includes the contribution of the core-width parameter a_0 , as it modifies the elastic strain energy in the framework of the non-singular dislocation theory. The second term accounts more specifically for the contribution of the dislocation core energy via the parameter ζ_{core} . Indeed, as revealed in Figure (4), this contribution contributes significantly to the dislocation line tension and cannot be neglected when modeling phenomena involving dislocations curvature like the Orowan process. The following modified Orowan equation is the outcome of fits made with more than 1000 simulations run with different parameters.

$$\tau_{Orowan} = \frac{\mu b}{L} \frac{A}{2\pi} \left[1.23 \left(\ln \frac{\bar{D}}{a_0} - 0.18 \right) + \zeta_{core} \right] \quad (9)$$

The harmonic mean term of L and D appears in the numerator in conformity with the BKS model, while the core width parameter (a_0) appears in the denominator since τ_{Orowan} has an inverse dependence on this term. The additional right hand side term of the equation account for the linear contribution of the core energy to the Orowan process. As illustrated in Figure (7), prediction made with Equation (9) gives excellent results and a correlation factor better than 0.99 when considering all our simulation data.

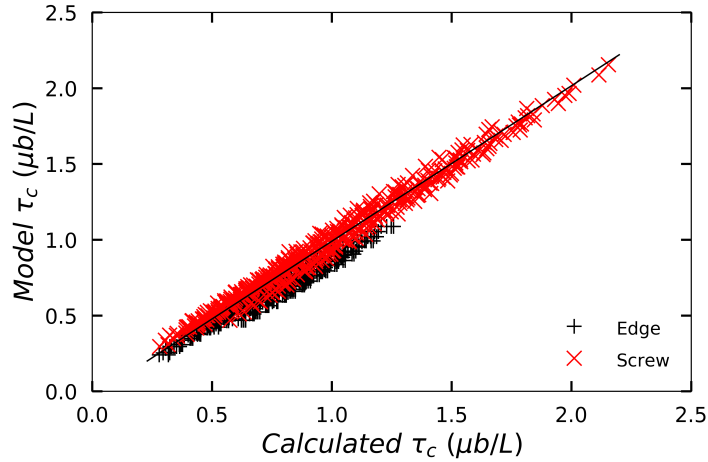


Figure 7: Comparison between simulation results and Equation (9) prediction for the 1000 combinations of parameters taken from Table (1) and tested in the present study.

It should be noted that Equation (9) is generic and can be used to interpolate any type of results on the Orowan mechanism. Thus, it becomes possible to perform a reverse analysis to identify the parameters of a DD simulation that can reproduce experimental data or other simulation results. In the following, an example of such adjustment is given. Equation (9) is used to define the parameters that are needed in our DD simulation to reproduce the results on the Orowan stress obtained by Lehtinen *et al.* with MD simulations [38]. These results are discussed and compared to the BKS model.

Lehtinen *et al.* studied the interaction between $1/2\langle 111 \rangle (11\bar{0})$ edge dislocation with non-coherent cementite precipitate (Fe_3C) of different spacing using molecular dynamics. These calculations were produced using the interatomic potential H13 proposed by Henriksson *et al.*

describing the FeCrC system [39]. Parameters that can be directly shared between MD and DD simulations are $\mu = 75$ GPa, $\nu = 0.379$ at $T = 750$ K, $b = 0.2502$ nm and obstacle diameter $D = 2$ nm. Use is then made of Equation (9) to identify the missing parameters needed in the DD simulations to correctly fix the dislocation strain energy and to be in agreement with the prediction of the interatomic potential used in the MD simulations. Such adjustment gives for the dislocation core width parameter $a_0 = 4.5$ nm and for the dislocation core energy parameter $\zeta_{core} = 0.51$. Both parameters value are physically meaningful and allow running DD simulations to either reproduce quantitatively the MD simulation results in a few seconds or to upscale the MD simulation results. To illustrate this point, a comparison is made in Figure (8) between the initial results of Lehtinen *et al.*, the results we obtained with the adjusted DD simulation and the BKS model predictions.

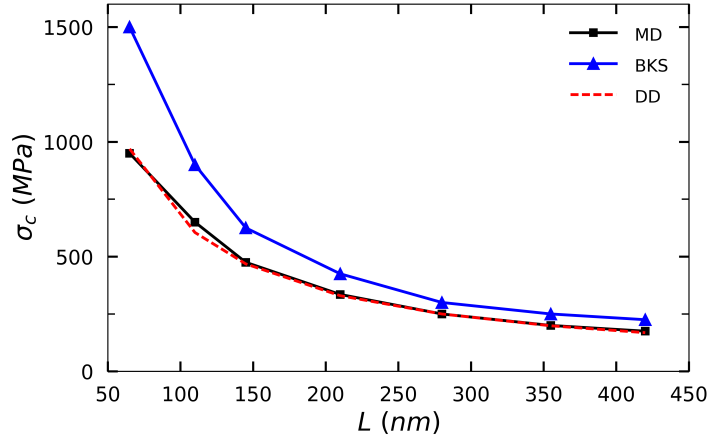


Figure 8: Comparison between critical Orowan stress as function of the inter-obstacle distance L for obstacle of $D = 2$ nm found using MD and BKS model and DD model in Equation (9). DD simulation parameters are $a_0 = 4.5$ nm, $\zeta_{core} = 0.51$.

The results of DD simulations when parametrized with the help of Equation (9) show an excellent match with the Orowan stresses computed with MD simulations. More precisely, the difference between the stress found in DD and MD simulations at different obstacles spacing is on average less than 2.4%. It is worth noting also that this difference is 53% between the BKS model and the MD simulation results. Such a difference could be interpreted as coming from the existence of thermally activated phenomena in the MD simulations that cannot be reproduced with any approach based only on the elastic theory. Our study, rather suggests that the dislocation strain energy that controls the dislocation dynamics in the MD simulations is simply different from the definition used initially in the BKS model.

To conclude, it should be noted that the parameterization of the dislocation strain energy in the framework of the non-singular dislocation theory is governed by the idea that the total dislocation energy should remain unchanged when changing the regularization amplitude. Hence, when increasing the dislocation core width parameter in a DD simulation (to avoid using tiny time steps), the dislocation core parameter is usually also increased to keep the total energy constant. As illustrated by our study, such solution without a systematic investigation of the parameterization effect could be problematic. Indeed, we show that the dislocation dynamics are

not affected in a simple manner by both parameters. For instance, some new DD simulations to be published in a forthcoming paper have shown that when modeling the interaction between a dislocation and radiation-induced loop defects, a drastic effect is observed on the dislocation dynamics by changing a_0 a few percent. Such parameterization change may even lead to the modeling of very different contact reactions.

In summary, a large dispersion is observed in DD simulation results depending on the choice of parameters used to control the dislocation strain energy. Such uncertainty has to be eliminated so that DD simulation results can be compared with MD and DD simulations or even experiment. A parametric study is proposed to incorporate the effect of essential simulation parameters in an equation form useful to predict the Orowan stress. This model reveals the existing coherence between the many simulations we performed and provides the means to calibrate rigorously future DD simulations. The model was tested and validated by a direct comparison with MD simulations. This work opens the door to more quantitative comparison between DD simulations and other simulation technics.

Acknowledgments

This work was performed in the framework of SOTERIA project funded by the European Union's "Horizon 2020" research and innovation program under agreement GA number 661913. The authors wish to thank Dr. Ghiath Monnet (EDF, Les Renardières) for the fruitful discussions.

References

- [1] L. Kubin, *Dislocations, Mesoscale Simulations and Plastic Flow*, Vol. 5, Oxford University Press, 2013.
- [2] J. P. Hirth, J. Lothe, *Theory of dislocations*, Krieger Pub. Co, 1982.
- [3] V. Bulatov, W. Cai, *Computer Simulations of Dislocations*, Vol. 3, Oxford University Press, 2006.
- [4] R. Peierls, The size of a dislocation, *Proceedings of the Physical Society* 52 (1) (1940) 34.
- [5] R. Miller, R. Phillips, G. Beltz, M. Ortiz, A non-local formulation of the peierls dislocation model, *Journal of the Mechanics and Physics of Solids* 46 (10) (1998) 1845–1867.
- [6] W. Cai, A. Arsenlis, C. R. Weinberger, V. V. Bulatov, A non-singular continuum theory of dislocations, *Journal of the Mechanics and Physics of Solids* 54 (3) (2006) 561–587.
- [7] A. Arsenlis, W. Cai, M. Tang, M. Rhee, T. Ooppelstrup, G. Hommes, T. G. Pierce, V. V. Bulatov, Enabling strain hardening simulations with dislocation dynamics, *Modelling Simul. Mater. Sci. Eng.* 15 (6) (2007) 553. doi: 10.1088/0965-0393/15/6/001.
URL <http://stacks.iop.org/0965-0393/15/i=6/a=001>
- [8] E. Martinez, J. Marian, A. Arsenlis, M. Victoria, J. Perlado, Atomistically informed dislocation dynamics in fcc crystals, *Journal of the Mechanics and Physics of Solids* 56 (3) (2008) 869–895.
- [9] P.-A. Geslin, R. Gatti, B. Devincere, D. Rodney, Implementation of the nudged elastic band method in a dislocation dynamics formalism: Application to dislocation nucleation, *Journal of the Mechanics and Physics of Solids* 108 (2017) 49–67. doi:10.1016/j.jmps.2017.07.019.
URL <http://www.sciencedirect.com/science/article/pii/S002250961730248X>
- [10] M. Boleininger, T. D. Swinburne, S. L. Dudarev, Atomistic-to-continuum description of edge dislocation core: Unification of the peierls-nabarro model with linear elasticity, *Physical Review Materials* 2 (8) (2018) 083803.
- [11] N. Ghoniem, M. S.-H. Tong, L. Sun, Parametric dislocation dynamics: a thermodynamics-based approach to investigations of mesoscopic plastic deformation, *Physical Review B* 61 (2) (2000) 913.
- [12] H. M. Zbib, T. D. de la Rubia, M. Rhee, J. P. Hirth, 3d dislocation dynamics: stress-strain behavior and hardening mechanisms in fcc and bcc metals, *Journal of Nuclear Materials* 276 (1-3) (2000) 154–165.
- [13] D. Weygand, L. Friedman, E. Van der Giessen, A. Needleman, Aspects of boundary-value problem solutions with three-dimensional dislocation dynamics, *Modelling and Simulation in Materials Science and Engineering* 10 (4) (2002) 437.
- [14] B. Devincere, R. Madec, G. Monnet, S. Queyreau, R. Gatti, L. Kubin, Modeling crystal plasticity with dislocation dynamics simulations: The 'micromegas' code, *Mechanics of Nano-objects* (2011) 81–100.

- [15] www.numodis.fr.
- [16] R. De Wit, The Self-Energy of Dislocation Configurations Made up of Straight Segments, *physica status solidi (b)* 20 (2) (1967) 575–580.
- [17] E. Orowan, Discussion on internal stresses, 1948, pp. 451–453.
- [18] E. Nembach, E. Nembach, Particle strengthening of metals and alloys, Wiley New York, 1997.
- [19] D. J. Bacon, Y. N. Osetsky, Dislocation—obstacle interactions at atomic level in irradiated metals, *Mathematics and Mechanics of Solids* 14 (1-2) (2009) 270–283.
- [20] D. J. Bacon, U. F. Kocks, R. O. Scattergood, The effect of dislocation self-interaction on the orowan stress, *Philosophical Magazine* 28 (6) (1973) 1241–1263. doi:10.1080/14786437308227997.
URL <http://dx.doi.org/10.1080/14786437308227997>
- [21] V. Mohles, E. Nembach, The peak-and overaged states of particle strengthened materials: computer simulations, *Acta materialia* 49 (13) (2001) 2405–2417.
- [22] G. Monnet, Investigation of precipitation hardening by dislocation dynamics simulations, *Philosophical Magazine* 86 (36) (2006) 5927–5941.
- [23] S. Queyreau, G. Monnet, B. Devincere, Orowan strengthening and forest hardening superposition examined by dislocation dynamics simulations, *Acta Materialia* 58 (17) (2010) 5586–5595.
- [24] G. Monnet, Multiscale modeling of precipitation hardening: Application to the Fe–Cr alloys, *Acta Materialia* 95 (2015) 302–311.
- [25] A. J. E. Foreman, The bowing of a dislocation segment, *Philosophical magazine* 15 (137) (1967) 1011–1021.
- [26] D. Terentyev, G. Bonny, C. Domain, R. C. Pasianot, Interaction of a $1/2\langle 111 \rangle$ screw dislocation with Cr precipitates in bcc Fe studied by molecular dynamics, *Physical Review B* 81 (21) (2010) 214106–214106.
- [27] F. Granberg, D. Terentyev, K. O. E. Henriksson, F. Djurabekova, K. Nordlund, Interaction of dislocations with carbides in BCC Fe studied by molecular dynamics, *Fusion Science and Technology* 66 (1) (2014) 283–288.
- [28] D. Hull, D. J. Bacon, Introduction to dislocations, Butterworth-Heinemann, 2001.
- [29] G. Monnet, D. Terentyev, Structure and mobility of the $1/2\langle 111 \rangle$ edge dislocation in bcc iron studied by molecular dynamics, *Acta Materialia* 57 (5) (2009) 1416–1426.
- [30] B. Devincere, Three dimensional stress field expressions for straight dislocation segments, *Solid state communications* 93 (11) (1995) 875–878.
- [31] G. Po, M. Lazar, N. C. Admal, N. Ghoniem, A non-singular theory of dislocations in anisotropic crystals, arXiv:1706.00828 [cond-mat]ArXiv: 1706.00828.
URL <http://arxiv.org/abs/1706.00828>
- [32] Y. Li, C. Robertson, M. Shukeir, L. Dupuy, Screw dislocation interaction with irradiation defect-loops in α -iron: evaluation of cross-slip effect using dislocation dynamics simulations, *Modelling and Simulation in Materials Science and Engineering* 26 (5) (2018) 055009.
- [33] A. Keyhani, R. Roumina, S. Mohammadi, An efficient computational technique for modeling dislocation–precipitate interactions within dislocation dynamics, *Computational Materials Science* 122 (Supplement C) (2016) 281–287. doi:10.1016/j.commatsci.2016.05.036.
URL <http://www.sciencedirect.com/science/article/pii/S0927025616302713>
- [34] X. J. Shi, L. Dupuy, B. Devincere, D. Terentyev, L. Vincent, Interaction of $1/2\langle 100 \rangle$ dislocation loops with dislocations studied by dislocation dynamics in α -iron, *Journal of Nuclear Materials* 460 (2015) 37–43. doi:10.1016/j.jnucmat.2015.01.061.
URL <http://www.sciencedirect.com/science/article/pii/S0022311515000781>
- [35] D. Terentyev, L. Malerba, D. J. Bacon, Y. N. Osetsky, The effect of temperature and strain rate on the interaction between an edge dislocation and an interstitial dislocation loop in α -iron, *J. Phys.: Condens. Matter* 19 (45) (2007) 456211. doi:10.1088/0953-8984/19/45/456211.
URL <http://stacks.iop.org/0953-8984/19/i=45/a=456211>
- [36] D. Terentyev, P. Grammatikopoulos, D. J. Bacon, Y. N. Osetsky, Simulation of the interaction between an edge dislocation and a $\langle 100 \rangle$ interstitial dislocation loop in α -iron, *Acta Materialia* 56 (18) (2008) 5034 – 5046. doi:<http://dx.doi.org/10.1016/j.actamat.2008.06.032>.
URL <http://www.sciencedirect.com/science/article/pii/S1359645408004527>
- [37] S. Queyreau, J. Marian, M. R. Gilbert, B. D. Wirth, Edge dislocation mobilities in bcc Fe obtained by molecular dynamics, *Phys. Rev. B* 84 (6) (2011) 064106. doi:10.1103/PhysRevB.84.064106.
URL <http://link.aps.org/doi/10.1103/PhysRevB.84.064106>
- [38] A. Lehtinen, F. Granberg, L. Laurson, K. Nordlund, M. J. Alava, Multiscale modeling of dislocation-precipitate interactions in Fe: From molecular dynamics to discrete dislocations, *Phys. Rev. E* 93 (2016) 013309–013309. doi:10.1103/PhysRevE.93.013309.
URL <http://link.aps.org/doi/10.1103/PhysRevE.93.013309>
- [39] K. Henriksson, C. Bjorkas, K. Nordlund, Atomistic simulations of stainless steels: a many-body potential for the fe–cr–c system, *Journal of Physics: Condensed Matter* 25 (44) (2013) 445401.